J Mater Sci (2006) 41:7150–7158
DOI 10.1007/s10853-006-0925-7

Microwave annealing for preparation of crystalline hydroxyapatite thin films

Daniel Adams · Gerald F. Malgas · R. D. Smith · S. P. Massia · T. L. Alford · J. W. Mayer

Received: 18 October 2004 / Accepted: 22 December 2005 / Published online: 8 October 2006

Abstract A sol was spun on single crystal silicon substrates at a spin-rate of 3000–5000 rpm followed by a low temperature cure to form a stable sol–gel/silicon structure. Good quality crystalline HA films of thickness ~300–400 nm were obtained by annealing the sol–gel/Si structure in a conventional cavity applicator microwave system with a magnetron power of 1300 W, frequency of 2.45 GHz, and at a low processing temperature of 425 °C for annealing times ranging from 2–60 min. X-ray Diffraction and FTIR analysis confirmed that the crystalline quality of the thin films were comparable or better than those heat-treated under the same processing conditions (temperature and time) in a Rapid Thermal Annealing (RTA) system. The RBS data suggests a composition corresponding to stoichiometric hydroxyapatite $Ca_{10}(PO_4)_6(OH)_2$, the major inorganic component of bone. The results showed that the HA film thickness decreases with increasing sol spin-rate. The HA films showed good biocompatibility because little monocyte adhesion occurred and hence no inflammatory response was activated in vitro. The potential of microwave annealing for rapid and low temperature processing of good crystalline quality HA thin films derived from sol–gel is demonstrated.

D. Adams (✉)
Department of Physics, University of the Western Cape, Private Bag X17, Bellville 7535, South Africa
e-mail: dadams@uwc.ac.za

G. F. Malgas
CSIR Materials Science and Manufacturing, P. O. Box 395, Pretoria 001, South Africa

R. D. Smith · S. P. Massia
Department of Bioengineering, Arizona State University, Tempe, AZ 85287-9709, USA

T. L. Alford · J. W. Mayer
Department of Chemical and Materials Engineering, Arizona State University, Tempe, AZ 85287-6006, USA

Introduction

Hydroxyapatite (HA) is widely preferred as the biomaterial coating of choice in both dental and orthopaedic implants due to its favourable osteo-conductive and bioactive properties [1]. Sol–gel synthesis of HA offers a viable alternative to the high temperature thermal spray method, which is currently used for biomedical applications [2]. It is difficult to control the microstructure of HA coatings prepared by thermal spraying [3]. Apart from the significantly lower processing temperatures, the sol–gel method also gives improved chemical homogeneity, better structural integrity, and improved stoichiometry. This affords the opportunity to form thin film coatings in a rather simple process and the ability to coat complex shapes [3, 4].

Sintering of sol–gel derived HA films under vacuum environment is frequently required to avoid oxidation of the supporting metal substrate, but at the expense of the structural stability of the HA coating [3]. Microwave heat treatment therefore becomes a viable option because it is performed in air.

Microwave heating differs fundamentally from conventional heating in that heat energy is generated from within the material instead of originating from

the outer surface [5]. As a result of this internal and volumetric heating in the microwave process, the thermal gradients and the flow of heat is opposite to that in materials processed by conventional heating [5]. These characteristics of microwave processing, make it possible to heat both small and large shapes very rapidly and uniformly; to process materials at lower surface temperatures; to reduce thermal stresses that cause cracking during processing; to process materials very rapidly (2–50 times faster than conventional processing); to perform selective heating; to synthesize new materials and microstructure; and to densify materials at low temperature with minimum grain growth (accelerated sintering) [5]. A comprehensive list of the characteristics and advantages of microwave processing is given in [5].

Recently, microwaves have been used to sinter nano-sized HA powder compacts in a house-hold microwave oven [6]. The microwaves coupled with the low temperature, synthesized nanocrystalline compound very effectively, and a sintered density as high as 95–98% was obtained for sintering times ranging from 5–15 min. In order to get similar densification in gel cast samples, temperatures above 1000 °C were required when ordinary furnace sintering was employed [7, 8]. Fang et al. demonstrated that transparent, pure phase hydroxyapatite ceramics (crystal size ~0.2 μm) could be fabricated by microwave processing at ambient pressure [9]. This was achieved by using a fine crystalline hydroxyapatite powder synthesized hydrothermally as starting material.

Compared to the microwave-induced sintering of HA powder as mentioned above, the present work is new because it describes the successful crystallization of sol–gel derived HA thin films. The results of the microwave-annealed samples are compared with those of samples, which had been heat treated in a rapid thermal annealing furnace. The primary focus of this study is therefore to demonstrate that microwave annealing can be used to obtain good quality HA films at temperatures as low as 400 °C.

Experimental

The precursor sol was formed by mixing a hydrated solution of *N*-butyl acid phosphate with calcium nitrate tetrahydrate dissolved in 2-methoxyethanol. The stoichiometric ratio of calcium to phosphorous in the coating solution was made the same as in HA, namely Ca:P = 1.67:1. The precursor sol prepared for this study had a molar concentration of 0.15 M. Details of the process can be found elsewhere [10, 11].

In this study we selected silicon (Si) as substrates for the HA coatings. Si was selected (i) to facilitate the use of the analytical techniques chosen and (ii) to obtain geometrically configured titanium substrates via photolithographic patterning of silicon for follow-up experiments involving a study of the response of osteoblasts to micro-topography in the HA/Titanium system. Prior to the coating process the Si substrates were cleaned in sequence with acetone, methanol and de-ionized water for a duration of 5 min. The sol was spun onto the cleaned Si substrates at spin-rates varying from 3000 to 5000 rpm for 10 s in air. The spun on sol films will be referred to as the ''deposited'' films through this report. The hygroscopic nature of the sol precursor necessitates that the initial films be spun on under relative humidity conditions of about 20–30%. Immediately after deposition, the films were dried on a hot plate at temperatures ranging from 50 to 250 °C for times up to 60 min. Following the drying step, the films were sintered in a cavity applicator microwave system with a magnetron power of 1300 W, frequency of 2.45 GHz, and at a power level of 50% for times ranging from 2–20 min. Throughout this report, the post-drying anneal will be referred to as ''sintering'' of the thin films. The microwave oven was fitted with a Raytek Infra-red (IR) sensor with the capability to measure the temperature over a range of –40 to 600 °C. Calibration of the temperature sensor showed that the best temperature profile is obtained at a power level of 50% because in this case the temperature rapidly increases at a ramp rate of 10.8 °C/s over the first 30 s and stabilizes at a maximum of about 425 °C (Fig. 1). For the microwave system used in this study the temperature could not be changed, therefore we

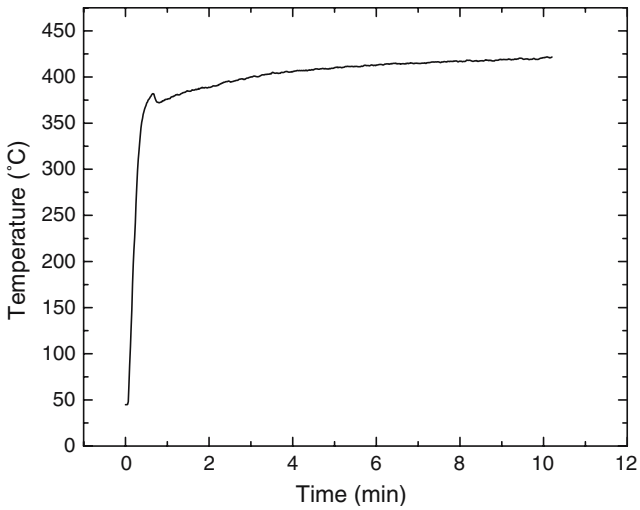

Fig. 1 The temperature versus time profile for microwave annealing at 50% power

investigated the effect of time on the HA film properties such as thickness and crystallinity. For the time-dependent studies the spin-rate was kept constant at 4000 rpm. For comparison purposes samples were also sintered in a glow-lamp rapid thermal annealing (RTA) furnace in an argon atmosphere. In order to compare the results from the microwave sintering with that from RTA, both anneals were carried out at the same temperature (~425 °C) and time (between 2 and 20 min).

The X-ray diffraction (XRD) analysis used to identify the HA phases was performed on a Philips X'Pert MPD diffractometer using Cu Kα radiation at a working voltage of 45 kV and filament current of 40 mA. A 1° glancing angle for the incident beam was used to analyze the films. The scan speed was 0.015/s. The obtained XRD spectra were compared with the Joint Committee on Powder Diffraction Standards (JCPDS) to identify the compounds [12]. The effective crystal size of the HA thin films, which is inversely proportional to the diffraction peak width was determined by using the Scherrer equation [13]:

$$\Delta(2\theta) = 0.9\lambda/D\cos(\theta) \quad (1)$$

where $\Delta(2\theta)$ represents the peak width at half-maximum intensity, λ is the wavelength for CuK_α ($\lambda = 0.154$ nm), and D is the effective crystal size in nanometers. Therefore, narrower peaks will indicate increased crystallinity for the same area under the curve.

Rutherford backscattering spectrometry (RBS) using 2.0 and 3.0 MeV He^{+2} ions respectively, was used to determine the film thickness and composition. The thickness and composition values were obtained by using the RUMP simulation program to simulate the RBS data [14].

An IFS 66v/s Harrick GATR infrared spectrometer using attenuated total reflectance (ATR) in transmission mode was used to perform the FTIR spectroscopy analysis. The Fourier Transform Infra-red (FTIR) system used a Mercury Cadmium Telluride (MCT) detector. A background subtraction was performed by subtracting the spectrum of an uncoated piece of silicon wafer from all specimen runs, each recorded spectrum being the average of 1024 scans. The FTIR chamber was evacuated to a pressure of 1 mbar to minimize water absorption onto the films. FTIR compared to XRD has three outstanding features that make it a useful technique to study thin HA films [11]. Firstly, the absorption bands corresponding to the phosphate and hydroxyl groups are sufficiently intense to provide strong signals in very thin films; secondly, the strong temperature dependence of the absorption bands also provides evidence for the refinement of the crystal structure even beyond the point where XRD indicates that the HA structure is complete and thirdly; FTIR measurements require surface areas of a few square millimetres, while the area needed for XRD is hundreds of times larger (~5 cm^2).

The biocompatibility of the HA coatings was evaluated in terms of monocyte adhesion. A live/dead cell assay test was used to determine the monocyte adhesion to the HA coating. The substrates were cleaned in 5 ml of acetone for 20 min. A further cleaning in a 5 ml of 5% Alconox detergent and then in distilled water followed this. Finally the substrates were rinsed three times with PBS in a sterile environment and placed in one of the six well plates. Monocyte cells were suspended in 3 ml of suspension. The substrates were then seeded with 1 ml of suspended monocyte cells. The staining solution was prepared and provided 1 ml of solution per 5×10^5 cells. Four microlitre of DiOC stock solution was added to 1 ml of culture media. The cells were incubated for 30 min. The substrates were rinsed three times with PBS. Fluorescence microscopy was used to scan for adherent monocyte cells. The percentages of adherent cells were calculated.

Results

Figure 2 depicts the RBS spectra of the HA/Si structures, which were prepared from sol spun on at three

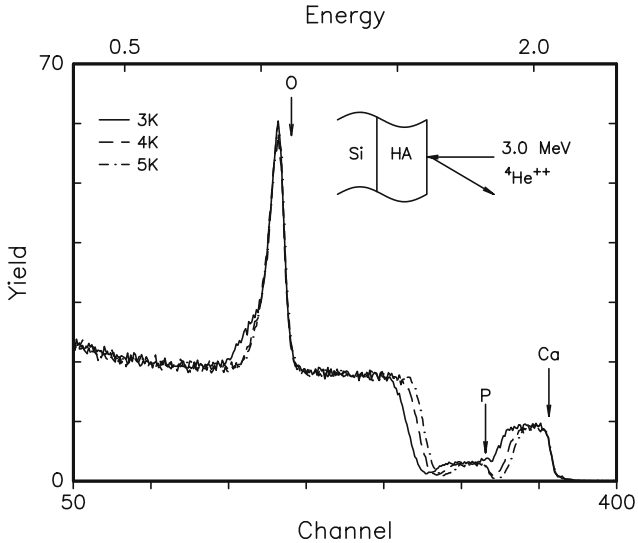

Fig. 2 The 3.0 MeV RBS spectra of HA thin films prepared from a sol spun on at three different spin-rates and microwave sintered at 425 °C for 20 min

different spin-rates (3000, 4000, 5000 rpm, respectively), dried and subsequently microwave annealed at 425 °C for 20 min. It is evident from the results that thicker HA films are formed as the spin-rate is decreased. At a spin-rate of 3000 rpm, the HA film is not just the thickest, but it also appears to be slightly non-uniform in thickness. The corresponding XRD spectra of the HA/Si structures, prepared in the same way as above are presented in Fig. 3. The peaks present were identified as (002), (102), (210), (211), (300), (202), (310), (222), (213), (321), (004), and (322) which are identical to those of standard HA [12], indicating the formation of an apatitic structure. Table 1 shows the HA film thickness and effective crystal size as a function of spin-rate for the samples annealed at 425 °C for 20 min. The (002) reflection was used in Eq. 1 to obtain the crystal size. The thickness was obtained from RUMP simulation of the data presented in Fig. 2. The data in Table 1 indicate that the spin rate affects the HA film thickness but has no significant effect on the effective crystal size.

Figure 4 shows the RBS spectra of the HA films obtained from microwave annealing for 2 and 20 min, respectively. The spin-rate for the deposited films in both spectra was 4000 rpm. The RBS signals indicate that the HA films are uniform in thickness. RUMP simulation of the data confirmed that the ratio of Ca/P is ~1.67, and the thickness of the films is ~350 nm. Apart from a slight difference in peak height, there is no significant difference between the samples annealed at these times. It is therefore, clear that the annealing time has no significant influence on the HA film thickness.

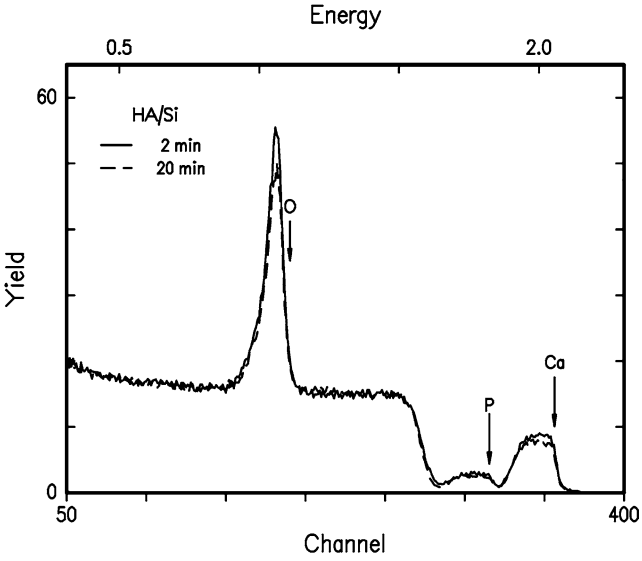

Fig. 4 The 3.0 MeV RBS spectra of HA thin films microwave sintered at 425 °C for 2 and 20 min, respectively. The sol was spun on at 4000 rpm

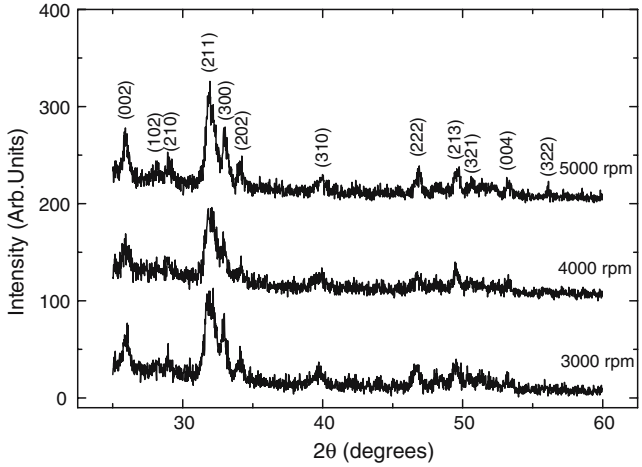

Fig. 3 XRD patterns of HA thin films prepared from a sol spun on at three different spin-rates and microwave sintered at 425 °C for 20 min

Table 1 HA film thickness and effective crystal size as a function of spin-rate for samples annealed at 425 °C for 20 min

Spin-rate (rpm)	Thickness (nm)	Effective crystal size (nm)
3000	425.0	19.25
4000	350.0	19.13
5000	325.0	19.62

The data was obtained by applying Eq. 1 to the (002) reflection in Fig. 3

Figure 5 shows the XRD spectra of the HA/Si samples, which has been microwave annealed at about 425 °C for 20, 30, and 60 min, respectively. The peak

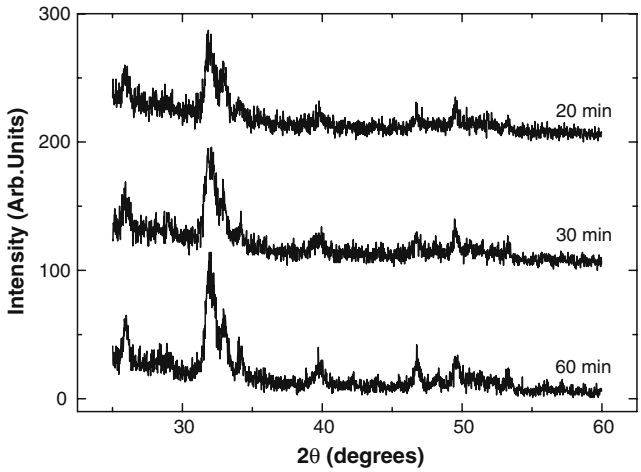

Fig. 5 XRD patterns of HA thin films prepared from a sol spun on at a spin-rate of 4000 rpm and microwave sintered at 425 °C for 20, 30, and 60 min, respectively

labels are the same as that indicated in Fig. 3. For these samples the sol was spun on at 4000 rpm for 10 s. By annealing the samples for 20, 30 and 60 min, respectively, the effective crystallite sizes (as determined by using Eq. 1) were 19.13, 22.59 and 25.87 nm. The data from the time-dependent studies therefore suggest that the effective crystal size of the HA films increases with annealing time.

Infrared spectroscopy was employed to provide information on the composition and chemistry of the thin films in terms of the functional groups present. It was also used to characterize the crystal structure of the coatings. This technique proved to be more effective in analyzing the crystallinity of submicron thin films than conventional X-ray diffraction. The FTIR data together with the band designations for the HA/Si samples spun at 4000 rpm and microwave annealed at 425 °C for 2 and 20 min, respectively are presented in Fig. 6. The major FTIR absorption bands in HA can be attributed to PO_4, CO_3, OH, and H_2O [15]. The phosphate stretching bands, ν_3 (triply degenerate) are located in the vicinity of 1000 cm^{-1} and the ν_4 (triply degenerate) absorption bands, corresponding to the bending motion in the phosphate ion are near wave number 600 cm^{-1}. The intensity of the bands near 1000 and 600 cm^{-1} is higher for the samples annealed for 20 min than at 2 min. It has been shown that vibrations due to the presence of the carbonate ion (CO_3^-) in sol–gel derived HA formulations are normally located at 1450 and 850 cm^{-1} [16]. Within the detection limits of the instrument no significant contributions from CO_3^- could be detected in the samples. The very low-intensity bump at 850 cm^{-1} (Fig. 6) may suggest the presence of an insignificantly small amount of carbonate. It has been reported that these bands disappear at higher temperatures because the carbonate converts to carbon dioxide (CO_2) and leaves the film [11, 17, 18].

To compare the effectiveness of the microwave annealing to induce crystallization of the sol–gel derived HA, samples were also sintered using rapid thermal annealing (RTA). In Fig. 7, the XRD pattern for the deposited samples is compared with those sintered with microwaves and rapid thermal annealing for 20 min. The peak labels are the same as that indicated in Fig. 3. By comparing the spectrum of the as-prepared sample with the annealed ones, it is evident that both annealing techniques caused crystallization of the HA coatings. Both the microwave and RTA annealed samples match the standard HA peaks [12]. The effective crystal size of the microwave annealed sample is 19.13 nm compared to 17.58 nm for the RTA annealed sample. Figure 8 shows the ν_4 PO_4^{3-} absorbance spectral region (500–650 cm^{-1}) for the HA samples annealed with microwave radiation and RTA, respectively for 20 min. This data was also used as a measure of the crystallinity of the samples sintered by both techniques. The peak heights A and B and the trough height C relative to the baseline were used to express the crystallinity in terms of the so-called, ''splitting factor'' (SF).

The biocompatibility of the HA films was evaluated in terms of monocyte adhesion to the HA substrate. Live/dead assays revealed that monocytes did not adhere to the HA coating. This is depicted in the fluorescent microscopy images in Fig. 9a–d. The images

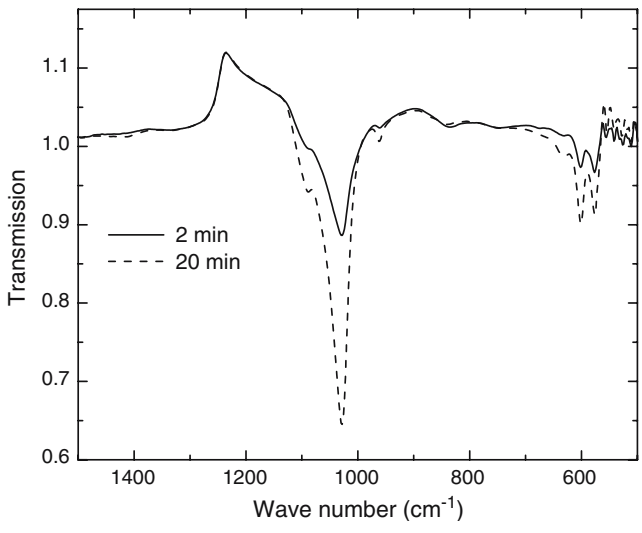

Fig. 6 Infrared transmission spectra of HA thin films microwave sintered at 425 °C for 2 and 20 min, respectively. The ν_3 (near 1000 cm^{-1}) and ν_4 (near 600 cm^{-1}) PO_4^{3-} bands are clearly visible

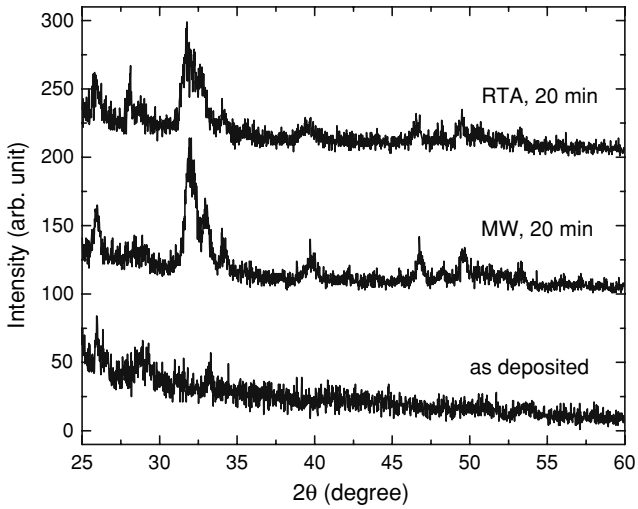

Fig. 7 XRD patterns of the as-deposited thin films are compared with those microwave and RTA sintered at 425 °C for 20 min

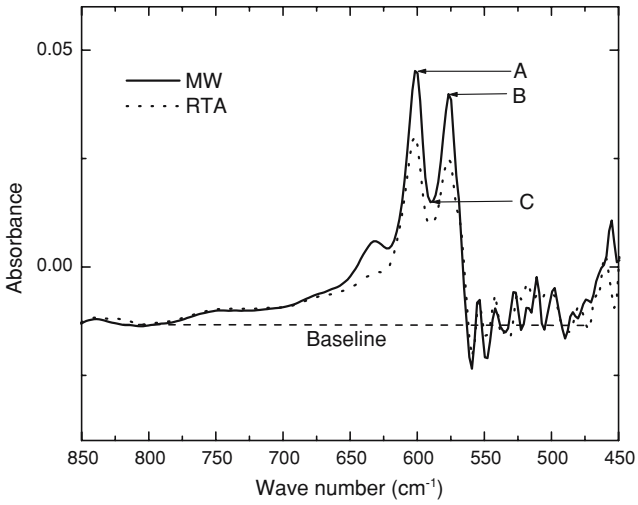

Fig. 8 Infrared absorbance spectra of HA thin films sintered at 425 °C for 20 min using microwave radiation and RTA heating, respectively. Only spectra of the v_4 PO_4^{3-} region are shown

were taken from the same area; and demonstrated that the wash removed almost all the monocytes. Figure 10 shows the extent to which monocyte adhesion has taken place and is obtained by counting the adherent cells in the captured images. Thirty minutes after monocyte suspension, the pre-washed surface had an average of eight monocytes per image. Fewer monocytes were floating after the PBS wash with 28% remaining. Very few monocytes were left on the dry surface with 10% remaining.

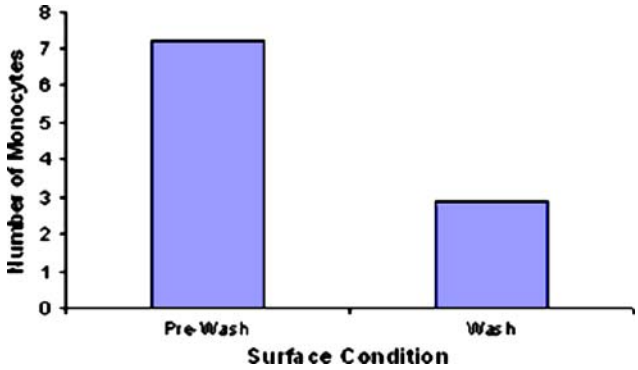

Fig. 10 A graph of the number of adherent monocytes counted in the captured images. Fewer monocytes were floating after PBS wash

Discussion

Bornside et al. [19] divide the spin coating process into four stages: deposition, spin-up, spin-off and evaporation, although evaporation may accompany each of the other three stages as well. During spinning a film arrives at its final thickness after sufficient evaporation has occurred, at which stage the film has become so thin and viscous that its flow stops [20]. Meyerhofer's spin coating model separates the spin-off and evaporation stages, and gives the final thickness as [21]

$$H_{\text{final}} = (1 - \rho_{\text{Ai}}/\rho_{\text{A}})(3\eta e/2\rho_{\text{Ai}}\omega^2)^{1/3} \quad (2)$$

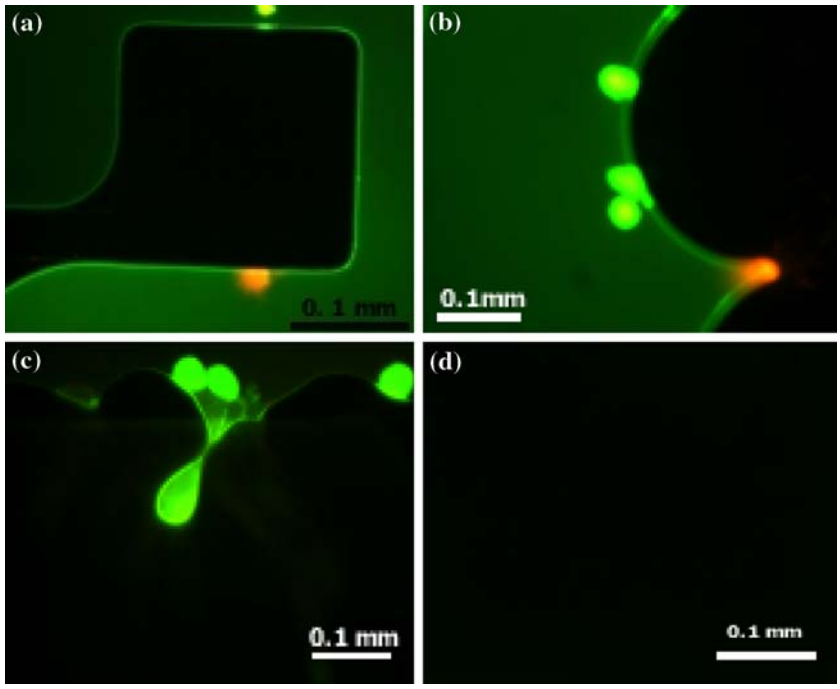

Fig. 9 Fluorescent microscopy images (**a–d**) indicating that a PBS wash removed most of the monocytes

where ρ_A is the mass of the volatile solvent per unit volume, ρ_{Ai} its initial value, and e the evaporation rate, ω the angular velocity and η the viscosity. From Eq. 2 it follows that the dependence of the HA film thickness on the spin-rate is reflected through the angular velocity (ω); since $H \propto (1/\omega^2)^{1/3}$, when the other factors are held constant. The higher the spin-rate the larger the angular velocity and hence the thinner is the film. Our results supported the theory, because the thinnest HA films were obtained at spin-rates of 5000 rpm. Lopatin further showed that for spin rates >3000 rpm, there is little decrease in the film thickness. It was shown that in fact, the thickness stays almost constant and thinner films are only formed if a sol of lower molar concentration is used [11]. The formation of stable sol–gel spun films demonstrated that a degree of polymerization occurred during film formation. However, the requirement of a heating step immediately after spinning implied that the degree of polymerization of the film is low, and thus the heating step serves to further polymerize the film [11]. The results suggested that the HA thickness is not influenced by the sintering time which implies that the polymerization step during film formation is an energy activated process.

The RBS results show that the films consist mainly of the elements P, Ca, and O. RUMP simulation of the data suggested a composition corresponding to stoichiometric hydroxyapatite $Ca_{10}(PO_4)_6(OH)_2$, the major inorganic component of bone [22]. From Fig. 4 the drop in the peak heights of the O and Ca in the RBS spectra is believed to be due to the formation of pores as a result of the evaporation of organics during the annealing steps and/or due to micro-cracks in the films [3, 23]. Once a sol–gel derived solid is formed during the drying step it still contains residual water from the condensation reactions and other molecules contained in the initial solution. It is therefore necessary to process the solid at elevated temperatures to drive off the excess volatiles and liquids to obtain the desired structure. Water strongly absorbs 0.195 and 2.45 GHz microwaves and, thus it is very efficiently heated at these frequencies [5]. It is also well known that microwave drying is particularly effective in removing low water contents (<5%) via volumetric heating. It is therefore anticipated that microwave annealing may be a more efficient way to remove residual water from the thin films.

The XRD results for the films that were microwave sintered at 425 °C revealed that significant crystal growth occurred within the first 20 min, whereas after this period growth is much slower (Fig. 5). The XRD results of the microwave-annealed samples show sharper peaks and greater peak heights compared to those, which had undergone RTA heat treatment, and therefore suggest enhanced grain size as well as crystallinity. Within the detection limits of the instruments used (FTIR and XRD) other crystalline phases such as CaO, and tricalcium phoshate (TCP) or amorphous-calcium phosphate could not be detected in any of the samples annealed by both methods. Some of these compounds are undesirable due to their fast dissolution in vivo.

Generally the v_3 PO_4^{3-} (900–1200 cm^{-1}) and v_4 PO_4^{3-} (500–650 cm^{-1}) spectral regions are used as the index of crystallinity, perfection, and ordering for bone [24]. In this study these contours were used to evaluate the crystallinity of the HA thin films. For the 20 min microwave anneals, the v_3 band at 1028 cm^{-1} is more intense and sharper than that for the 2 min. This behaviour indicates that the samples microwave-annealed for the longer times have a better crystalline structure. This result was also confirmed by the data obtained from the v_4 band.

Termine and Posner [25] used infrared studies of bone apatite to define the so-called ''percent crystallinity'' in known concentrations of synthetic amorphous and crystalline apatites to express crystallinity. The ''percent crystallinity'' is measured as a peak-splitting function calculated as a ratio of the areas above and below the double peak of the phosphate anti-symmetric bending frequency (v_4) at approximately 550–650 cm^{-1} [15]. The greater the separation or split of the double peak the better is the crystallinity. Weiner and Bar-Yosef [26] defined a ''splitting factor (SF)'' as a measure of crystallinity. The SF is calculated by summing the heights of the peaks A (601 cm^{-1}) and B (576 cm^{-1}) and dividing this value by the height of the trough C between them (Fig. 5). All the heights are measured relative to a common baseline. Therefore, the splitting factor, is given by

$$\mathrm{SF} = \frac{A + B}{C}, \tag{3}$$

where A and B are the peak heights and C is the trough height relative to the baseline [26].

Based on the data presented in Fig. 5, splitting factors of 3.83 and 3.48 were calculated for the HA samples annealed with microwave and RTA, respectively. The calculated SF data therefore indicate that the microwave annealing results in a better crystalline quality HA film than the RTA results. This conclusion is in agreement with the data obtained from the XRD analysis.

The final crystalline state of the films is dictated by the microstructural changes that occur during processing of the samples [11]. Processing involves three critical stages, namely, (i) gellation, to form a semi-rigid structure as a result of polymerisation of the spun-on sol (spinning step); (ii) amorphisation or formation of a porous structure from the gel, during the drying step or removal of excess solvents; and (iii) densification and crystallization, which occurs during the sintering step. This step involves the elimination of the porous structure and removal of any residual organics. It has however, been shown that spun-on films subjected to increased drying temperatures, that is, accelerated aging before the sintering step, exhibited a significantly lower crystallization growth rate [27]. This effect however, becomes less significant at higher sintering temperatures. The reason for the reduced crystallization growth rate is because cross-linking of the molecules occurs during the drying stage, and a condensed and stiff phosphate structure (P–O–P bonds) is formed from the condensation reaction of the H_3PO_4 molecules in the hydrated precursor sol [27]. As the drying temperature increases the rate of cross-linking also presumably increases. When HA is formed the network must be re-arranged to form the apatite structure, with calcium and hydroxyl ions arranged in the channels formed between the columns of the phosphate ions [27]. The activation energy for the breakage of the P–O–P bond ranges from 83.7 to 167.4 kJ/mol [28], and is a function of the position of the bond and environmental factors. Elevated sintering temperatures are therefore required to break the P–O–P bonds in order to form HA. It is believed that the barrier to formation of crystalline HA at lower temperature is the need to break the P–O–P bonds in the amorphous precursor structure.

In this study it was found that the films were not completely dry after spinning at rates 3000–5000 rpm and the films tended to form droplets if left at room temperature for a few minutes. In addition to this, films dried at temperatures <250 °C or for short times appeared hazy, which was due to the presence of tiny droplets on the surface. However, even at higher drying temperatures and longer times, the films turn hazy while being dried under conditions where the relative humidity is more than 30%. Films dried at ~250 °C for 60 min and under relative humidity conditions of $<30\%$ had mirror-like surfaces. According to Lopatin et al. [29] the droplets are composed of solvent that has not been driven off, and form when the cooling film contracts and forces the solvent to the surfaces.

If the evaporation is not rapid enough, gellation may not be completed at the end of the spin cycle; resulting in the film not being rigid enough to withstand the tensile forces that results in droplet formation. It is believed that the hygroscopic nature of the solvents makes the spinning process very sensitive to the humidity conditions; in the sense that at high humidity levels the evaporation process is slowed-down. High relative humidity levels therefore contribute to the inhibition of the gellation step and hence could prevent the formation of a sufficiently rigid gel structure. Therefore, higher drying temperatures (~250 °C) were used to ensure the formation of stable films prior to sintering. This was, however done at the expense of obtaining small grain size HA films during sintering.

To evaluate the quality of the microwave sintered HA, the coatings were subjected to a biocompatibility test in vitro. The HA thin films were stable in the biological environment in which they were tested. Fluorescence microscopy used to scan for monocyte adhesion indicated that the HA coatings did not cause an inflammatory response. Due to electrochemical changes, the HA coating would resist macrophage induction and active oxygen species, which normally results from phagocytosis caused by an inflammatory response [30]. A reduction of the active oxygen species would increase resistance to deleterious corrosion of metal implants.

This paper forms part of an ongoing study, which investigates HA thin film properties such as porosity and morphology, as well as modelling the sintering mechanism of microwave annealing of sol–gel derived coatings. Meek [31] suggested that microwave fields and power density are significantly intensified in the porous regions of a ceramic material. When dense regions begin to form, the microwave field begin to decouple from these regions and couple more strongly with the regions of low density and low relative dielectric constant. This property of microwave annealing will also be exploited to obtain uniformly densified HA thin films.

Conclusion

Sol–gel-derived HA thin films of good crystalline-quality have been obtained by microwave annealing in a cavity applicator system (1300 W, 2.45 GHz) at a temperature of about 425 °C and power level of 50%. XRD and FTIR confirmed that the phase of the hydroxapatite corresponds to that of standard HA. When compared with the results from RTA, the microwave-annealed samples showed a better crystalline quality. It has been demonstrated that microwave annealing offers an alternative method over

conventional heating for short times and low temperature processing, and improved microstructure of HA films.

Acknowledgements The authors would like to acknowledge the financial support of the National Research Foundation (South Africa)—Grant numbers: 2053829 (EGIC) and 2050587 (URDP), University of the Western Cape and Arizona State University (ASU). The work is partially supported by the NSF (USA), to whom the authors are greatly indebted. A word of thanks is also due to Shawn Whaley (Department of Chemistry, ASU) for the assistance with the FTIR analysis. We gratefully acknowledge the use of facilities within the Center for Solid State Science at ASU.

References

1. Corpe RS, Steflik DE, Whitehead RY (2000) Crit Rev Biomed Eng 28:395
2. Haddow DB, James PF, Van Noort R (1998) J Sol-gel Sci Tech 13:261
3. Liu D, Troczynski T, Tseng WJ (2001) Biomaterials 22:1721
4. Chai CS, Ben-Nissan B, Pyke S, Evans L (1995) Mater Manuf Process 10:205
5. Sutton WH (1989) Ceram Bull 68(2):76
6. Vijayan S, Varma H (2002) Mater Lett 56:827
7. Fang Y, Agarwal DK, Roy DM, Roy R (1992) J Mater Res 7:490
8. Varma HK, Sivakumar R (1996) Mater Lett 29:57
9. Fang Y, Agrawal DK, Roy DM, Roy R (1995) Mater Lett 23:147
10. Russell SW, Luptak KA, Suchicital CTA, Alford TL, Pizziconi VB (1996) J Am Ceram Soc 79(4):37
11. Lopatin CM (1999) PhD Thesis, Arizona State University
12. Powder diffraction File, Joint Committee on Powder Diffraction Standards (JCPDS), Card No. 9-432, 1994
13. Cullity BD (1967) Elements of X-ray diffraction. Addison Wesley, Read, MA, p 99
14. Doolittle LR (1985) Nucl Instrum Methods Phys Res B9:344
15. Surovell TA, Stiner MC (2001) J Archaeol Sci 28:633
16. Layrolle P, Ito A, Tateishi T (1998) J Am Ceram Soc 81:1421
17. Manso M, Langlet M, Jimenez C, Martinez-Duart JM (2001) Int J Inorg Mater 3:1153–1155
18. Hwang K, Song J, Kang B, Park Y (2000) Surf Coatings Technol 123:252–255
19. Bornside DE, Macosko CW, Scriven LE (1987) J Imaging Tech 13:122–129
20. Brinker CJ, Scherer GW (1990) Sol–gel science Academic Press, Boston, MA
21. Meyerhofer D (1978) J Appl Phys 49:3993
22. Spivak JM (1990) J Biomed Mater Res 24:1121
23. Hwang K, Lim Y (1999) Surf Coatings Technol 115:172
24. Miller LM, Vairavamurthy V, Chance MR, Mendelsohn R, Paschalis EP, Betts F, Boskey AL (2001) Biochim Biophys Acta 1527:11
25. Termine JD, Posner AS (1996) Nature 211:268
26. Weiner S, Bar-Yosef O (1990) J Archaeol Sci 17:187
27. Lopatin CM, Pizziconi VB, Alford TL (2001) J Mat Sci Mat Med 12:767
28. Van Wazer R 1958 Phosphorous and its compounds. Interscience Publishers, Inc, NY, p 515
29. Lopatin CM, Pizziconi V, Alford TL, Laursen T (1998) Thin Solid Films 326:227
30. Smith RD (2004) Masters Thesis. Arizona State University
31. Meek TT (1987) J Mater Sci lett 6:638